Real-time trace detection of security-relevant compounds in complex sample matrices by thermal desorption-single photon ionization-ion trap mass spectrometry (TD-SPI-ITMS) Spectrom...

ARTICLE *in* ANALYTICAL AND BIOANALYTICAL CHEMISTRY · AUGUST 2009

Impact Factor: 3.44 · DOI: 10.1007/s00216-009-2916-4 · Source: PubMed

9 AUTHORS, INCLUDING:

Jasper Hölzer
Helmholtz Zentrum München
6 PUBLICATIONS **50** CITATIONS
SEE PROFILE

Michael Pütz
Bundeskriminalamt
48 PUBLICATIONS **900** CITATIONS
SEE PROFILE

Anal Bioanal Chem
DOI 10.1007/s00216-009-2916-4

ORIGINAL PAPER

Real-time trace detection of security-relevant compounds in complex sample matrices by thermal desorption–single photon ionization–ion trap mass spectrometry (TD-SPI-ITMS) Spectrometry (TD-SPI-ITMS)

Elisabeth Schramm · Jasper Hölzer · Michael Pütz · Rasmus Schulte-Ladbeck · Rainer Schultze · Martin Sklorz · Andreas Ulrich · Jochen Wieser · Ralf Zimmermann

Received: 30 April 2009 / Revised: 10 June 2009 / Accepted: 12 June 2009

Abstract For the detection of security-relevant substances at low concentrations in complex matrices, coupling of thermal desorption–single photon ionization–ion trap mass spectrometry (TD-SPI-ITMS) was successfully tested. The main advantage of taking solid samples with a wipe pad followed by thermal desorption is the low detection limit by enhanced vapor pressure. Single photon ionization is a soft ionization technique which reduces the target ion fragmentation and shields bulk components with high ionization energies (IE) like nitrogen yielding to clearly arranged mass spectra with significant high mass peaks. To obtain low false-positive and false-negative rates, especially necessary for security-relevant substances, the ion trap mass spectrometer allows identification of signals with MS/MS studies. In this concept, the soft ionization technique fits well with the MS/MS studies, as peaks with high masses are generated yielding significant MS/MS fragments. For the ionization, photon energies between about 8 eV (155 nm) and 12 eV (103 nm) were generated with electron-beam-pumped rare gas excimer lamps (EBEL). Depending on the rare gas used, light with different photon energy is generated, adapted to the substances of interest. So, even most narcotics, having relatively low IEs, can be ionized with 8.4 eV photons without massive fragmentation. For most explosives, photons with higher energy must be used as their IEs are higher. In this work, a mobile setup with a commercial ion trap mass spectrometer has been developed and tested. Even a first real-scenario measurement campaign was accomplished successfully proving the field-suitability of the system.

Keywords Single photon ionization · Security-relevant substances · Ion trap mass spectrometry · Trace detection · MS/MS · Excimer light source

E. Schramm · J. Hölzer · R. Zimmermann
Helmholtz Zentrum München, Institute of Ecological Chemistry,
Ingolstädter Landstraße 1,
85764 Neuherberg, Germany

E. Schramm · J. Hölzer · M. Sklorz · R. Zimmermann (✉)
University of Rostock,
Dr.-Lorenzweg 1,
18059 Rostock, Germany
e-mail: ralf.zimmermann@uni-rostock.de

M. Pütz · R. Schulte-Ladbeck
Federal Criminal Police Office (BKA),
Forensic Science Institute (KTI),
65173 Wiesbaden, Germany

R. Schultze · J. Wieser
Optimare GmbH,
Emsstraße 20,
26382 Wilhelmshaven, Germany

A. Ulrich
Physik Department E12, Technische Universität München,
James-Franck-Straße 1,
85748 Garching, Germany

Introduction

Real-time detection of security-relevant substances is important for many areas of application. One large area of interest is the trace detection of explosives and their precursors, e.g., at borders, airports, courthouses, and prisons to prevent terrorist attacks. At the same time, narcotics and their precursors are interesting to detect at these places, too. By repressing narcotic smuggling, it is possible to reduce drug-related crime and the financing of terroristic groups. Furthermore, trace detection is useful for the discovery of clandestine drug labs, which are often

Published online: 09 July 2009

dangerous places [1]. Landmines, which are another source of danger, can also be detected.

For all these applications, a detection system has to be reliable, fast, mobile, sensitive, and selective. The apparatus has to be able to be moved to the place of interest and be operable before long. The measurements themselves should last only a few minutes to get a real-time response. Additionally, it should be trouble-free to run to enable the operation by trained personnel.

Besides these requirements, the system has to be very selective and sensitive. One problem is that the vapor pressure at room temperature, especially of explosives, is rather low. The vapor pressure of the explosive trinitrotoluene (TNT) is, for example, about 5.93×10^{-6} hPa at room temperature [2], resulting in an equilibrium vapor concentration over pure solid substance of approximately 6 parts per billion (ppb). A common method to increase this concentration is to sample solid particles on wipe pads and desorb them at elevated temperature, shifting the gas/particle equilibrium and resulting in higher vapor concentrations.

Another problem, however, is that complex and potentially unknown matrixes are present. Desorbing solid particles, not only substances of interest were collected, but various other compounds like fats, dirt, etc. All these substances are desorbed, too, and they are likely present in much higher concentration than the substances of interest. Additionally, flushing gas for desorption is necessary. It is possible to use inert gases, but it would be much easier for field-use, if ambient, at most, dried air could be used.

However, different detection systems are commercially available and widely used. One is the combination of a thermal desorber and ion mobility spectrometry (IMS). It is used at many airports worldwide (e.g., Ionscan 400B, Smiths Detection plc., UK) [3]. The IMS technique is well suited for real-time detection due to its short response time and low detection limit. Additionally, IMS devices are mobile, small in size and more affordable than mass spectrometer (MS) systems. On the other hand, mass spectrometry (MS) systems are superior regarding selectivity and identification power and most IMS contain a radioactive Ni-63 source for ionization yielding complex use regulations. Another common combination is thermal desorption coupled to gas chromatography (GC) with chemiluminescence detection, also known as thermal energy analyzer. This technique is also used at many airports (e.g., EGIS, Thermo Scientific Inc., USA) [4]. A third example is GC combined with mass spectrometry (GC/MS) e.g., the MM 1 (Bruker Corp., USA) which has been mounted in military reconnaissance vehicles [5].

Besides the existence of these commercial products, the issue described above is still of great interest and many developments are in progress. Numerous different detection systems were applied on this field. According to Yinon [6] they can be sub-divided into three classes: vapor and particle detectors, radiation detectors, and biochemical detectors. In this paper, we concentrate on vapor and particle detection. Besides the most used IMS and GC-MS, additionally, gas sensors, different kinds of spectroscopy, electronic noses and of course canine detectors were applied amongst others. Further information can be found in following references: [7-11].

Here, we describe a new combination of three methods: Thermal desorption –single photon ionization–ion trap mass spectrometry (TD-SPI-ITMS). With this combination, several systems with their specific advantages were combined. Thermal desorption of wipe pads produces high vapor pressures of analytes. With SPI, soft ionization is accomplished [12, 13], and ion trap mass spectrometry makes selective and sensitive MS/MS studies possible [14-16]. All components will be described in detail below. First, conceptual results obtained with a home-built setup have already been published [17]. There, first fundamental experiments had been performed; whereas in this work, a setup with a commercial ion trap mass spectrometer is described. With this demonstrator, the necessary performance, user-friendliness, and field-capability have now been reached.

There are some examples where an SPI-ITMS technique has already been used with different light sources for different applications. Laser light of 118 nm wavelength (10.5 eV photons) were used by Hurst and coworkers [18]. They were generated by frequency-tripling of 355-nm light emitted from an Nd:YAG laser. Therewith, aromatics in automobile exhaust were analyzed in real time. Hanna et al. [19] investigated aerosols with an SPI-ITMS system based upon a tunable (7.4 to 10.2 eV photon energy), laser-based vacuum UV (VUV) light source. A microwave-excited H_2/He VUV lamp (121.6 nm, 10.2 eV) was used by Morii, Tsuruga, and coworkers [20-22] for their SPI-ITMS system. With it, they performed real-time analysis of polychlorinated dibenzodioxines within incinerator exhaust. All these ionizations occur within the vacuum of the ITMS, whereas Syagen et al. [23, 24] use discharge lamps for atmospheric pressure photo ionization [25, 26] and low-pressure photo ionization. The lamps provide photons between approximately 8 and 12 eV depending on the rare gas filling. However, due to the relatively high pressure, unwanted ion reactions like charge transfer due to ion collisions can occur.

There are also some examples, where SPI MS was used for explosive detection. Oser and coworkers [27, 28] used a laser-based VUV light source for SPI.

Our setup applies another VUV light source, the so-called electron-beam-pumped rare gas excimer lamp (EBEL). The working principle of this light source is described in detail in the "Experimental setup" section. The source can produce VUV photons with energies between 8.4 (148 nm) and 11.6 eV (107 nm) depending on the rare gas or rare gas mixture used [29, 30]. So, it is possible to

choose a photon energy which ionizes the security-relevant substances with ionization energies (IE) between 8 and 12 eV [31], and will not ionize most bulk components like nitrogen (IE=15.6 eV), oxygen (IE=12.1 eV), or water vapor (IE=12.6 eV) [32]. This results in soft ionization since only little excess energy is transferred to the molecule and good detection limits due to shielding of the matrix molecules. The EBEL sources produce very brilliant light (focusable to a spot size of about 1 mm^2) with relatively narrow energy distribution. Compared to lasers or microwave lamps, they are well suited for field-use, as no laser safety regulation has to be approved and no sophisticated adjustments are required. There are several publications with EBEL coupled to time-of-flight and quadrupole mass spectrometer [33, 34], but this is the first time the EBEL was coupled to an ion trap mass spectrometer enabling MS/MS studies.

Experimental method

The system for trace detection of security-relevant substances described in this work consists of three main components: The thermal desorber, the single photon ionization ion source, and the ion trap mass spectrometry section. In Fig. 1.1, a kind of flowchart of a measurement sequence is shown.

For a measurement, first a sample is taken with a PTFE wipe pad. This pad is put into the thermal desorber where the solid substances upon the pad are desorbed. Therewith, high concentrations in the vapor phase are reached. This is especially important for most explosives since their vapor pressure at room temperature is too low for detection. The desorbed molecules are guided through a heated capillary into the ion source, where they are ionized by VUV photons generated by the EBEL. This principle of single photon ionization is illustrated in Fig. 1.2. The molecules absorb one single photon. If the photon energy is higher than the IE of the molecule, ionization occurs and if the photon energy is much higher than the IE and even higher than the so-called appearance energy of the fragments, fragmentation occurs. Our goal is to use photon energies just above the ionization energies of the target molecules to get a preferably fragment-free ionization. As the IE is substance specific, our target photon energy depends on the substance of interest as illustrated by the green and red areas in Fig. 1.2. Additionally, the bulk gases, from which oxygen has the lowest IE of 12.1 eV, should not be ionized as indicated by the green area below 12.1 eV and red area above 12.1 eV in Fig. 1.2.

For example, the IE of 3,4-methylenedioxy-*N*-methylamphetamine (MDMA), the most important active substance in ecstasy tablets, is 7.5 eV [31]. For this substance, as for most narcotics, an EBEL source with krypton gas filling was used resulting in a photon energy of 8.4 eV (center of the energy distribution of the photons. In this case, as well as for other rare gases, the energy distribution has a full width at half maximum (FWHM) of about 0.8 eV). Thus, only little excess energy is transferred to the molecule, leading to ionization with little or ideally no energy left for fragmentation. This is preferable, like indicated by the green area above 7.4 eV in Fig. 1.2. Photons with 10.7 eV, emitted from an EBEL with a krypton/argon gas mixture, would fragment these substances heavily. Thus, the corresponding area in Fig. 1.2 is colored red. On the other hand, these photons are well suited for soft ionization of many explosives, for example TNT with an IE of 10.5 eV [31]. Of course, 8.4 eV photons are not suited for TNT detection, as the IE is too high so that it would not be ionized. These two examples show how the proper choice of the photon energy can

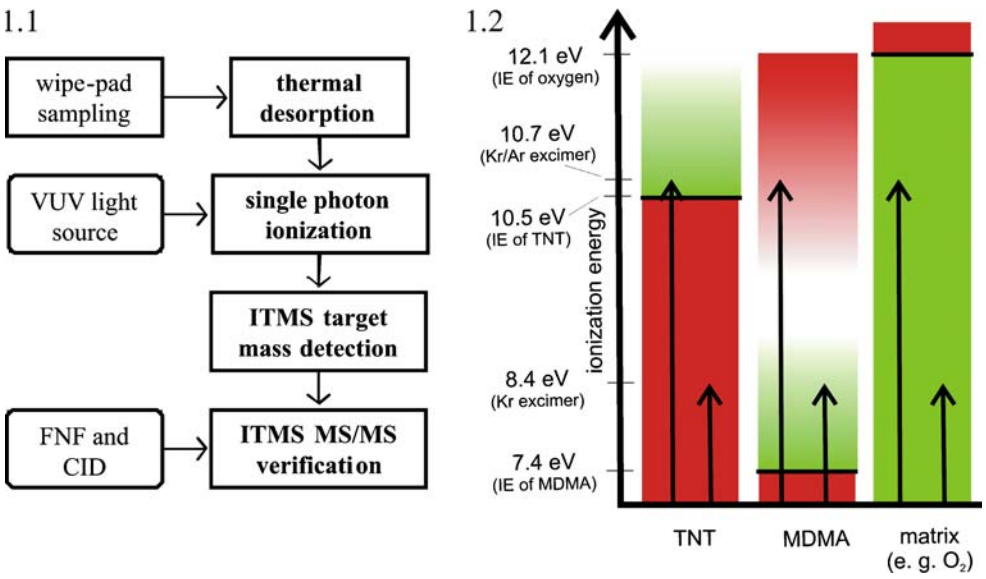

Fig. 1 *1* Flowchart of the measurement sequence and *2* sketch of the SPI ionization, data from [17]; (true to scale except the energy distribution of the excimer photons and the onset of the fragmentation)

provide ionization without much fragmentation. This is important, as peaks with high masses or even molecular ion peaks are preferred for the third component of our measurement setup, the detection of the ions with ion trap mass spectrometry.

This mass spectrometer system provides the possibility of MS/MS studies. Thereby ions with high masses, preferably molecular ions, which were ionized softly with SPI, were collected within the ion trap. Then, they were isolated by a so-called filtered noise field (FNF) and fragmented with collision induced dissociation (CID). Thus, the ions can be identified due to their fragmentation pattern with low false-positive and false-negative rates. As MS/MS is especially suited for high masses as the fragments are more significant, this matches well to the soft ionization. Also, the possibility to accumulate target ions within the ion trap fits well with our continuous light source and yields good sensitivity.

Experimental setup

For realizing the measurement method, first experiments were made with a first setup based upon a home-built ion trap [17]. This setup was used because of its flexibility, as all mechanical components were known and could be exchanged and the whole controlling software, based on a Labview (National Instruments Corp., USA) program, could be easily modified. With this setup, first conceptual measurements were made to demonstrate the proof-of-principle and to identify parameters which were important to modify. However, to get a more user-friendly system, a better performance as well as a more sophisticated data analysis program, a commercial ion trap mass spectrometer is now being used. For the new setup, the GCMS4000 (Varian Inc., USA) was chosen and modified. An overview of the setup is displayed in Fig. 2.

Figure 2.1 shows a mobile rack with an overall size of about 70 cm×120 cm×150 cm (height×width×depth) into which the whole system was mounted. This setup requires only external electric power as all peripheral equipment like helium supply, heater control, computer, forepump, and power supply (230 V AC, about 2 kVA) for the VUV light source were already integrated. Also, it is relatively resistant with regard to dust as it is cased and ventilated with filtered ambient air. Additionally, the pumps and heater produce heat, so that the setup is relatively resistant to cold environment conditions, too.

Further developments to minimize the setup can still be foreseen, as the EBEL and the thermal desorber are relatively small and several developments for a hand-held ion trap mass spectrometer were done in the past years [35].

Figure 2.2 gives an overview over the whole setup; each component will be described in detail in the following subsections.

Thermal desorption units

For thermal desorption of the wipe pads, two different desorption units were used, as shown in Fig. 2.2. The first one is the original thermal desorber from the ion mobility spectrometer Ionscan 400B (Smiths Detection plc, Watford, UK). With this system, the wipe pad is put into the desorber and a heated cartridge (250 °C) moves up to the wipe pad.

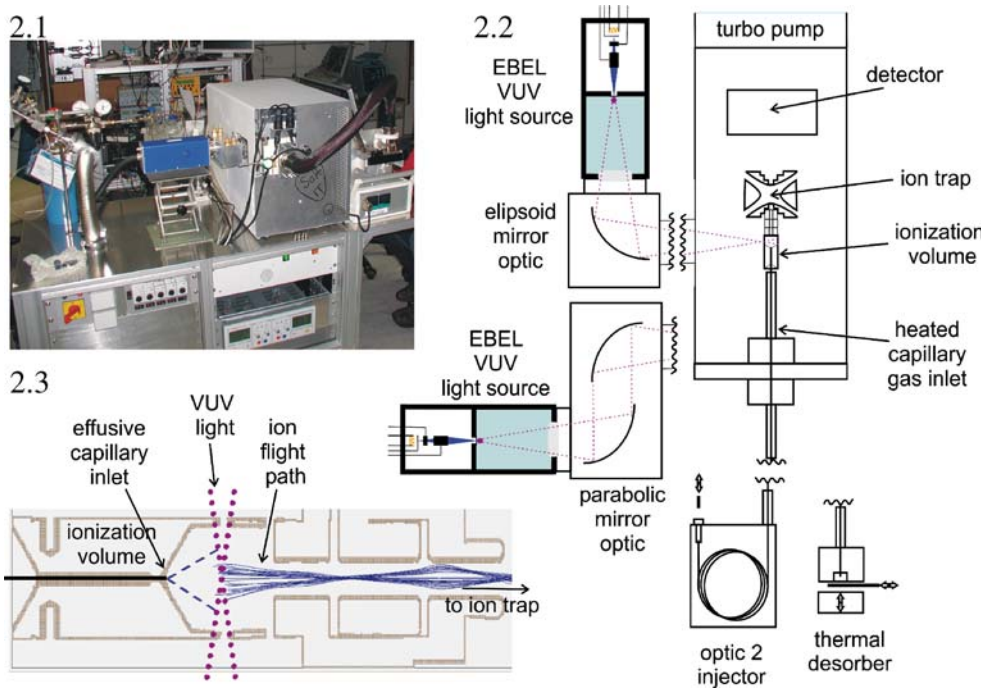

Fig. 2 Setup of the measurement system, *1* photograph of the demonstrator used in the field test, 2 schema of the measurement setup, *3* simulated ion flight path from the ion source to the ion trap

Thus, the pad is clamped between the cartridge and a newly constructed, heated adapter (250°C). The desorbed substances were sucked by the vacuum of the mass spectrometer into the deactivated fused silica capillary inlet, connected directly to the ion source (also heated up to 250°C). Thereby, 1 ml/min ambient air was sucked in as well. The dead volume of the adapter is about 1 ml. The other system used for desorption is the GC injection port Optic 2 (Shimadzu Europa GmbH, Duisburg, Germany). There, the same filters as used for the thermal desorber were cut into small stripes and put into the cold liner. Afterwards, they were flushed with helium and then heated up with 16 K/s to 250°C for thermal desorption. The injection port was also connected with the heated capillary transfer line to the ITMS.

The advantage of the thermal desorber is that it is already used at many airports worldwide and the suitability for field-use is well proven. However, the desorber is not vacuum-sealed and the adapter has a relatively big dead volume and stainless steel surfaces may catalyze thermal degradation of labile compounds. The injection port is not subject to these disadvantages, since it consists only of deactivated surfaces, is vacuum-sealed, and heated up quickly, so that the pad can be flushed with helium when it is still cold and the desorption can be performed under helium atmosphere. Thus, reaction with ambient air and reaction at surfaces can be minimized. Additionally, the dead volume is much smaller and better flushed, so that the peak form will be better. For all measurements, a constant flow of 2 ml/min helium was realized. The same setup coupled to a GC/MS-system was used by Schnelle-Kreis et al. [36] for routine thermal desorption of aerosol filters. Streibel et al. [37] used this injection port for direct thermal desorption/pyrolysis experiments in combination with a photo ionization time-of-flight mass spectrometer. However, as the injection port is not suited for field measurements due to the cumbersome pad handling, both systems came into operation.

VUV light source and mirror optics

After thermal desorption, the molecules are sucked through a heated transfer capillary and enter the ion source effusively. The ion source is shown in detail in Fig. 2.3. There, the molecules are ionized by SPI via VUV photons generated by the EBEL. The setup of the EBEL is shown in Fig. 2.2. It mainly consists of a vacuum chamber containing an electron gun (e-gun) and a chamber filled with rare gas ($p>1$ bar). Both are separated by a thin silicon nitride foil (0.7×0.7 mm^2; 300 nm thick). During operation, a 12-keV electron beam is generated by the e-gun and enters the rare gas through the silicon nitride foil. Due to the very small thickness of the foil, only a fraction of about 15% of the electron-beam energy is positioned within the foil, only a fraction of about 15% of the electron energy is deposited in the foil, the remaining fraction of the electron energy excites and ionizes the rare gas. Excited diatomic rare gas molecules (excimers) are formed via gas kinetic processes. Their radiative decay generates intense VUV radiation [38]. By using different rare gases or rare gas mixtures, it is possible to generate photons with different energies. The measurements described in this work were performed using krypton, argon, and a mixture of argon and krypton as the gas filling; these results in photon energies of 8.4 eV (150 nm), 9.8 eV (126 nm), and 10.7 eV (116 nm), respectively. As mentioned above, the photon energy is distributed around these center values with an FWHM of about 0.8 eV for all pure rare gases. The spectral stability is very good as the rare gas can be kept clean with a getter easily. The photon flux is very critical for the sensitivity of the system. For the measurements presented in this manuscript, a 3-μA emission current of the e-gun was used. This theoretically yields a continuous photon flux of 10^{13} to 10^{14} photons per second in the ionization region.

For focusing the photons into the ion source, two different mirror optics were used as shown in Fig. 2.2. The first one consists of two parabolic mirrors, but in the course of the development, a setup with only one ellipsoidal mirror was introduced and tested. Both focusing optics worked well but the ellipsoidal mirror has the advantage that only one mirror surface is used which reduces the reflection loss. Additionally, a larger solid angle can be used. The enhanced photons flux in the ion source improved the detection limit by about one order of magnitude. Especially for determining the detection limit, this new mirror optics version was used. The alignment of all mirrors was performed by an adjustable mirror mount with vacuum feed-through. The signal of the mass spectrometer can be used for optimization. So far, no long-time decrease of the mirror reflectivity was noticeable and the positioning of the mirrors endured transportation in the small van during the field measurement campaign.

Ion trap mass spectrometer and ion source

For the setup, a modified 4000GCMS (Varian Inc., USA) was used. For generating TD-SPI-ITMS, the ITMS was adapted for alternate use of SPI and EI. Therefore, the gas inlet was moved from the left-hand side to the front with a new front flange containing heated capillary feed-through and venting valve. The mirror optic and light source were connected at the left-hand side where the gas inlet has been (see Fig. 2.2). Additionally, the ion source was replaced with a new one shown in Fig. 2.3. The measurements were started with 65 ms ionizing the molecules entering the ion source, guide them into the ion trap, and store them there.

With this external ionization, the trapping efficiency is about 2%. For performing MS/MS studies, the molecules of interest were isolated with the so-called FNF and afterwards fragmented with the so-called CID. For further information about the principle of ion trap mass spectrometers, please refer to references [14-16]. Usually, a measurement rate of 1 Hz was used averaging two or three spectra internally.

One main innovation is the ion source displayed in Fig. 2.3. On the left-hand side, it is closed except for an aperture for the capillary with a diminution at the end for positioning of the capillary. On the opposite end, it is open to the ion lenses guiding the ions into the ion trap. Orthogonal to the gas flow, two apertures with 3 mm diameter at the top and the bottom in Fig. 2.3 serve as in- and outlet for the VUV light. In the original ion source, two apertures for entering of the electrons of the two filaments for EI are positioned orthogonally to both axes. In the modified version, one of these openings is closed. This enables the shielding of the electrons of one filament, so that it is possible to record SPI mass spectra without disturbing EI when choosing this filament by software. This enables easy software-driven switching between EI and SPI and even normal auto-tune routines can be performed in EI mode without any further hard- or software modifications.

To verify the performance, EI-MS measurements were taken under the same conditions before and after the modification. As test gas, nitrogen with each 10 parts per million (ppm) benzene, toluene, and xylene was used. The obtained mass spectra are as good as identical, showing that the modification does not influence the performance of the system. Additionally, the flight paths of the ions within the new ion source have been simulated using SimIon® (Scientific Instrument Services, USA). The results are shown in Fig. 2.3. For the simulation, the voltages of the lenses were set at the same values that were used for the measurements. The ion source itself is set on ground potential. The start point of the ions was set to the region where the effusive gas stream from the capillary crosses the VUV light ray (see Fig. 2.3). The simulated ions were single-charged and had a mass of 200 amu. The initial velocity of the ions was estimated to be about 310 m/s according to a kinetic energy of 0.1 eV. The direction of the initial ion movement was set as the vector between the end of the capillary and the origin of the ion with a random distribution with a half angle of 10°. The result shows that as good as all ions were extracted from the ion source and focused into the ion trap. This confirms that the modifications do not influence the performance of the system.

Results and discussions

To test the setup, first, some measurements were accomplished to compare the thermal desorber and the injection port. Afterwards, some measurements with explosives and narcotics were made with both systems. As the injection port is a rather perfect desorption unit, the detection limit of the whole setup was determined with this setup. However, measurements with matrix within the laboratory as well as the real-scenario measurement campaign were performed with the thermal desorber, as it is suitable for field-use contrary to the injection port.

Comparison of thermal desorber and injection port

For comparison and characterization of the two desorption units, measurements with pyrene (purity 99%, Sigma Aldrich Inc., USA) were performed. Pyrene has a boiling point of 394 °C, which is high above the temperature of the desorber units and inlet systems and is therefore well suited to demonstrate the desorption power of the two units and identify problems caused by absorption and dead volumes. The vapor pressure of pyrene at 250 °C is about 32 hPa and the IE is 7.4 eV [32], so for these measurements, a krypton-EBEL was used. In Fig. 3.1, the temporal evolution of the molecular ion peak of m/z=202 during desorption of 1 µg pyrene is displayed. All measurements were recorded with a measurement rate of 5 Hz, with the same method (ionization time of 65 ms, no averaging, krypton-EBEL with an e-gun emission current of 1 µA and equal substance amounts). Comparing the graphs for desorption with the Optic 2 injection port (Fig. 3.1a) and the one with the thermal desorber (Fig. 3.1d)), it is visible, that the integrated signal during the whole desorption is more or less independent, so no losses occur (about 30,000 counts), but the desorption within the injection port is much faster resulting in a briefer but much higher signal. When restricting desorption time to 1 minute to get fast measurements (like shown in Fig. 3.1b and c), the integrated signal from the thermal desorber averaged about 24,000 counts and therewith about 20% lower than the one from the injection port. That results from the incomplete desorption of pyrene in the thermal desorber due to dead volume, while using the injection port, the desorption is nearly finished after 10 s.

Another aspect is that the desorption profile from the thermal desorber depends on the spatial distribution of the substance onto the wipe pad. For Fig. 3.1b pyrene was put on the middle of the wipe pad and for Fig. 3.1c at the brim of the wipe pad. As can be seen in Fig. 3.1b, the signal is higher in the beginning as the pyrene desorbs just underneath the capillary. The signal afterwards and the signal of Fig. 6.1c results from the substance within the death volume above the wipe pad. Additionally, we suppose an adsorption and slower desorption of pyrene at the desorber head. The integrated signals are both in the same range.

In addition to the temporal profile of the desorption, the possible thermal fragmentation of security-relevant sub-

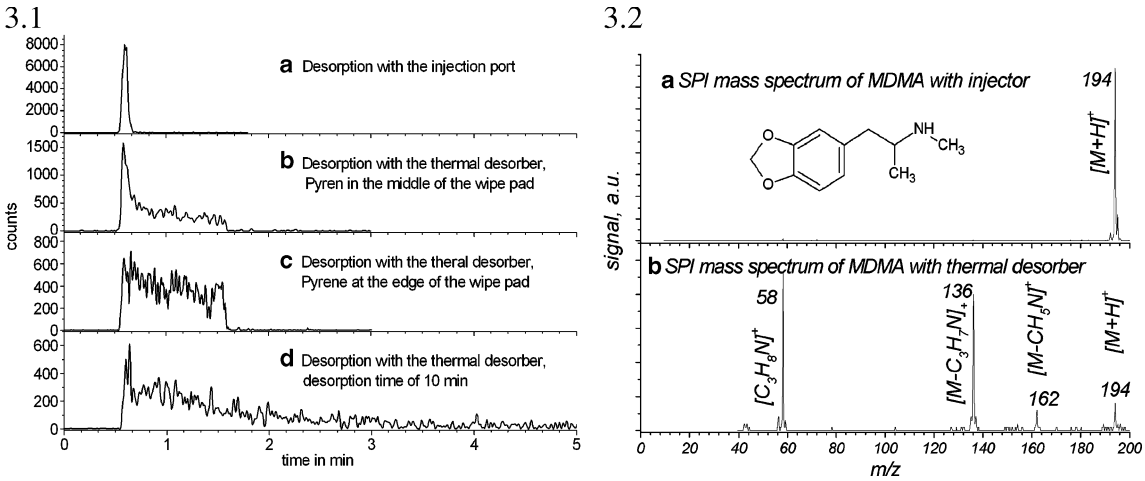

Fig. 3 *1* Temporal profile of the desorption of 1 µg pyrene with the thermal desorber and with the injection port. 2 MDMA SPI mass spectra with the injection port and with the thermal desorber

stances, which are mostly rather instable, was investigated. Therefore, the synthetic drug MDMA (3,4-methylenedioxy-*N*-methylamphetamine) was measured. MDMA is the main active substance in most seized ecstasy tablets. It belongs to the group of amphetamine-type stimulants and its chemical structure contains a beta-phenylethylamine moiety like some endogenous neurotransmitters. Its molecular mass is 193 amu. It was provided by the German Federal Criminal Police Office (BKA) with a purity of more than 99%.

Fig. 3.2 displays the SPI mass spectra of the desorption of MDMA with both thermal desorber units, as above, settings were constant. The mass spectrum with desorption in the injection unit (Fig. 3.2a)) shows significant lower fragmentation than the one recorded with the thermal desorber (Fig. 3.2b)). Also, the fragmentation pattern with the thermal desorber is not reproducible. This implies that the fragmentation already occurs within the thermal desorber due to the desorption in ambient atmosphere and the steel surface of the thermal desorber. In both mass spectra, the molecule ion appears at m/z=194, corresponding to M^++1. This results most likely due to the attachment of a hydrogen atom to the MDMA molecule within the trap. That is a common effect occurring inside the ion trap and does not really disturb the detection.

In summary, the injector port yields less fragmentation, higher absolute signal and therefore a drastic reduction of the detection limit. But, as mentioned above, it is not really applicable for field-use.

SPI mass spectra measured with the thermal desorber

With the thermal desorber, the narcotic heroin (diacetyl-morphine) and the explosive TNT (2,4,6-trinitrotoluene) were desorbed. Heroin (molecular mass 369 amu) is one of the most common worldwide traded narcotics and TNT is a widely distributed military explosive. Both substances were provided by the BKA with a purity of more than 95%.

In Fig. 4.1, the results for heroin were shown. For the SPI, an EBEL with krypton was used generating photon energy of 8.4 eV. In the SPI-ITMS mass spectrum of heroin, shown in Fig. 4.1a, the molecular ion peak is the base peak. Thus, the SPI mass spectrum shows lower fragmentation as the EI mass spectrum displayed in Fig. 4.1d. In Fig. 4.1b, the molecular ion is isolated and accumulated with the FNF. The MS/MS mass spectrum of the molecular ion peak (see Fig. 4.1c) shows a base peak with m/z=327 which results from the loss of a C_2H_2O-group and is the main peak of the EI mass spectrum. So, a peak at m/z=327 within an MS/MS study of m/z=369 is our indicator for heroin.

In Fig. 4.2, the results for TNT were shown. For the SPI, an EBEL with a krypton/argon mixture was used generating photon energy of 10.7 eV, as the IE of TNT is 10.5 eV. For TNT, the base peak of the SPI-ITMS mass spectrum (Fig. 4.2a) as well as of the EI mass spectrum (Fig. 4.2d) is the fragment with m/z=210 which results in the loss of an OH-group. Again, the fragmentation due to SPI is lower and the molecular ion peak bigger in relation to the fragments. Nevertheless, for MS/MS studies, the base peak was isolated (Fig. 4.2d). In Fig. 4.2c), the MS/MS mass spectrum of the peak at m/z=210 shows fragment peaks at m/z=164 and m/z=193. These peaks can be found in the EI mass spectrum, too, and results from the loss of an additional OH-group and an NO_2-group, respectively. So, these two peaks within the MS/MS mass spectrum are indicators for TNT.

The fragmentation of both substances with SPI is much lower than with EI enabling the MS/MS studies of the molecular ion peak or a main fragment at high mass. Nevertheless, lower fragmentation would yield higher

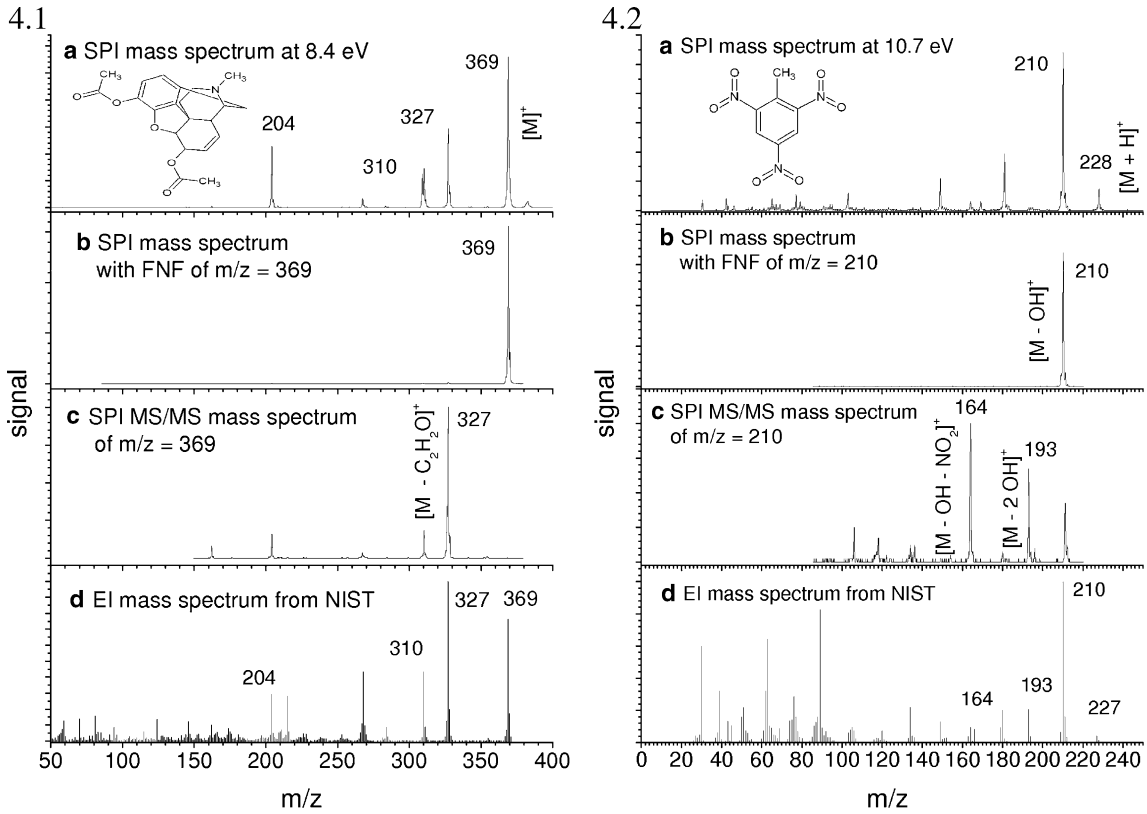

Fig. 4 SPI MS and MS/MS as well as for comparison the EI mass spectra of heroin (*1*) and TNT (*2*) with the thermal desorber

target peaks and therewith lower detection limits. In the future, we will try to cool the molecules before ionization with a supersonic molecular beam inlet. So, the internal energy of the molecules will be reduced and surplus energy minimized.

SPI mass spectra measured with the injection port

With the Optic 2 injection port measurements of MDMA (M=193 amu) and cocaine (M=303 amu) were performed. Both are common narcotics and both substances were ionized with photon energy of 8.4 eV for single photon ionization.

In Fig. 5.1, mass spectra of cocaine are shown. The SPI-ITMS mass spectrum (Fig. 5.1a)) shows a significant molecular ion peak, at m/z=304 which results from the attachment of an H-atom within the ion trap. Additionally, two fragment peaks were present at m/z=83 and m/z=182, which are even higher than the molecule ion peak. All three peaks are within the EI mass spectrum from NIST (Fig. 5.1e)), too, regarding the mass difference of 1 m/z due to the H-attachment. For MS/MS studies, the peak at m/z=304 was isolated (Fig. 5.1b) and fragmented resulting in a peak at m/z=182 (Fig. 5.1c). This peak can be isolated and fragmented subsequently resulting in an MS^3 mass spectrum. The peaks appearing in this mass spectrum are present in the EI mass spectrum, too, and can be labeled as shown in Fig. 5.1d.

The SPI MS mass spectra of MDMA shown in Fig. 5.2a exhibits only very small fragment peaks and a molecular ion peak an m/z=194. In the subsequent figures, the FNF, MS/MS, and MS^3 mass spectra are displayed (Fig. 5.2b–d). They all show reasonable peaks also present in the EI mass spectrum in Fig. 5.3e. In contrast to the SPI spectra, the EI fragment at m/z=58 is the base peak and the molecular ion peak is not visible. An identification of MDMA by this EI spectrum is not possible as the fragment at m/z=58 cannot be clearly assigned with MDMA but can be caused by, e.g., acetone from nail-polish remover and is often found at public transit terminals. The identification due to the MS/MS peaks, in the contrary is valid, the fragment at m/z=163 results from the loss of a CH_4N-group (nitrogen alpha cleavage), the one at m/z=135 result from the loss of the fragment with m/z=58 (C_3H_8N; benzyl cleavage).

Determination of the detection limit

For the determination of the detection limit of the setup, m=100 ng MDMA was desorbed several times with the Optic 2 injection port.

During desorption, SPI MS/MS mass spectra of the molecular ion at m/z=194 were measured. Therefore, two

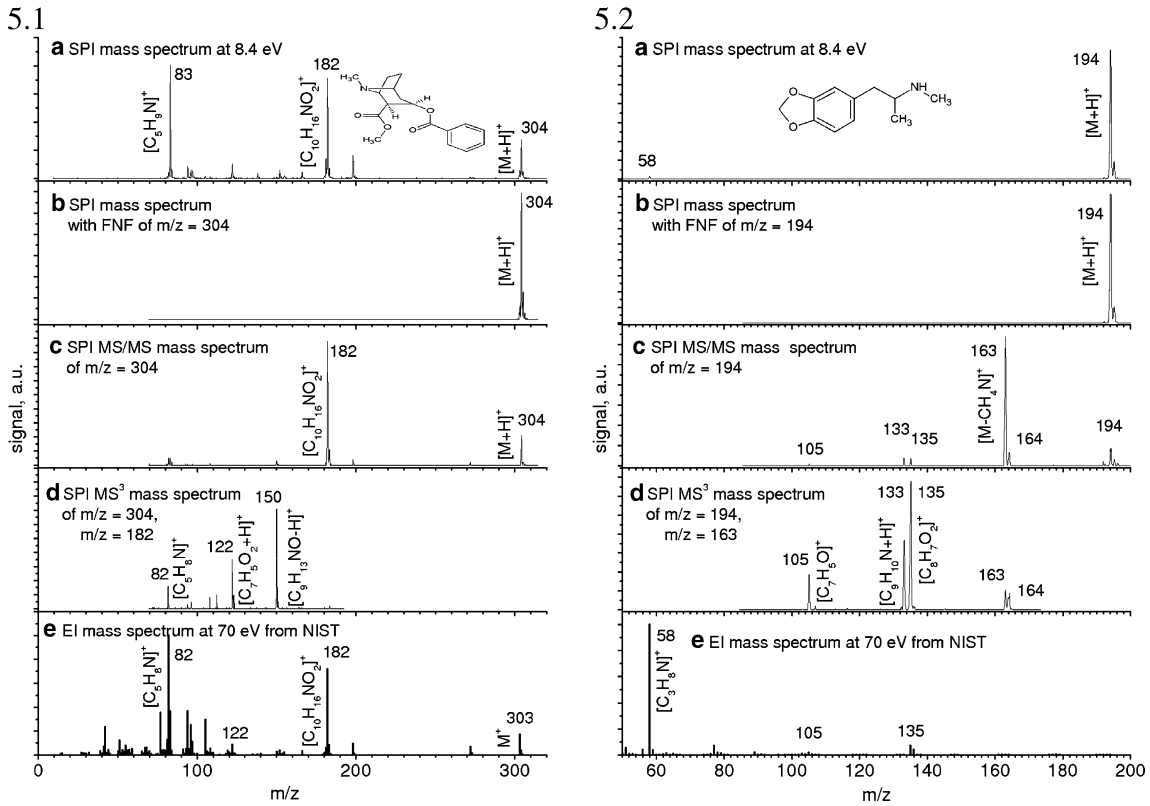

Fig. 5 SPI MS, MS/MS, and MS^3 as well as for comparison the EI mass spectra of cocaine (*1*) and MDMA (*2*) with injection port

measurements with 65 ms ionization time, respectively, were averaged resulting in a measurement rate of 1 Hz. The krypton-EBEL was connected with the ellipsoid mirror module and set to 3 μA emission current. The temporal profile of the expected MS/MS fragment at m/z=163 was shown in Fig. 6. For calculating the detection limit, the peak was integrated over desorption time and the noise of a blind desorption was integrated over the same time. Out of the integrated signal of S=92 counts and the noise of N= nine counts with a variance of σ=13 counts, a limit of detection of 32 ng was calculated according to [39]:

$$\mathrm{LOD} = 2 \times m \times \frac{\sigma}{S-B} = 2 \cdot 100\,\mathrm{ng} \cdot \frac{13\ \mathrm{counts}}{92\ \mathrm{counts} - 9\ \mathrm{counts}}$$

$$= \underline{32\,\mathrm{ng}}$$

This detection limit is about two orders of magnitude higher than the ones gained with IMS measurements [6]. However, there is some potential enhancing the limit of detection and even in this state, the system is suited for first real-scenario measurements (see below).

Results of matrix measurements with the thermal desorber

For field measurements, the matrix tolerance of the system is rather crucial as the complex and unknown matrix is one of the main challenges for such systems. To determine the matrix-acceptance of our system, some measurements with matrix were performed within the laboratory. For these experiments, the thermal desorber was used, as this is the system for field measurements.

To investigate reproducible, common, and difficult matrix, two different substances were chosen. The first one is lipstick. This was selected, as this is a typical substance present at any public transit terminal. As it consists mainly of paraffin, which have rather high molecular masses, not much noise signal is supposed. But it is a nice, demonstrative example for a typical matrix. The second one is diesel fuel as it contains many different hydrocarbons supposed to generate a massive noise signal. Additionally, some substances (especially not legal narcotics) were smuggled inside fuel canisters or car tanks so that it is a rather realistic matrix. One of the substances seized within car tanks is safrole. Safrole is the main component of sassafras oil, an extract of the sassafras tree used for production of MDMA. Thus, safrole was used as target substance for the matrix measurements. As safrole has an IE of 7.8 eV [31], photon energy of 8.4 eV was used for the matrix measurements. For these measurements, two scans with 65 ms ionization time each were averaged resulting in a measurement rate of 1 Hz. The substances were pipetted onto a wipe pad and desorbed for 1 min

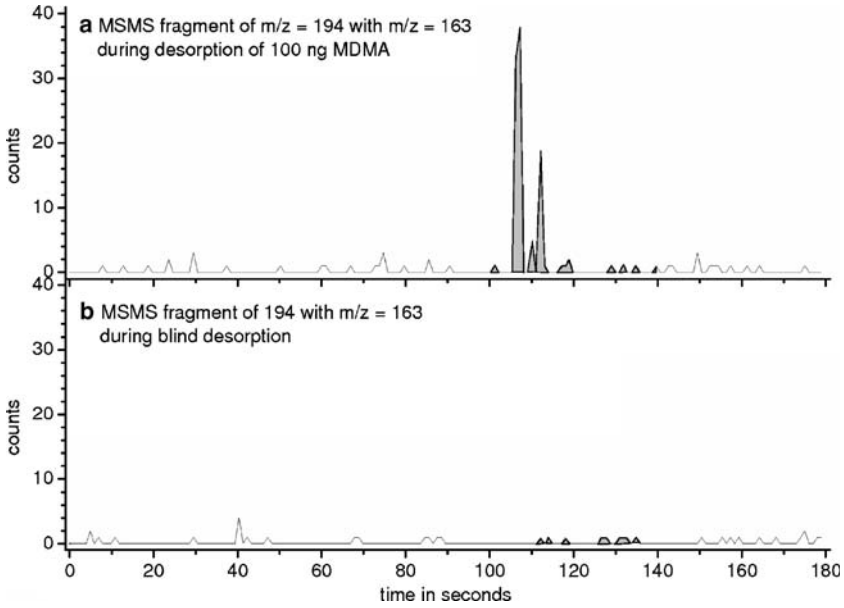

Fig. 6 Desorption of 100 ng MDMA with injection port and determination of detection limit

within the thermal desorber. The krypton-EBEL was set to 3 μA and connected with the ellipsoid mirror module.

In Fig. 7.1a and 2a, SPI-ITMS mass spectra of the two matrixes were shown. Thereby, the diesel fuel matrix shows quite many and high peaks, the lipstick produce much less noise, as expected. Afterwards, the same substances were measured with the MS/MS method for detection of safrole (molecule mass of 162 amu), which consists of enrichment, isolation and fragmentation of the peak at m/z=162. Thereby, the typical MS/MS fragments of safrole at m/z= 131 and 104 (which are within the EI mass spectrum from NIST in Fig. 7.1d and 2d, too) are not visible, thus, these matrices will not produce false-positive signals. In Fig. 7.2b), the lipstick-matrix (some mg) produce only small noisy signals (main peaks at m/z=103, 118, 133), the diesel fuel matrix in Fig. 7.1b shows a significant peak at

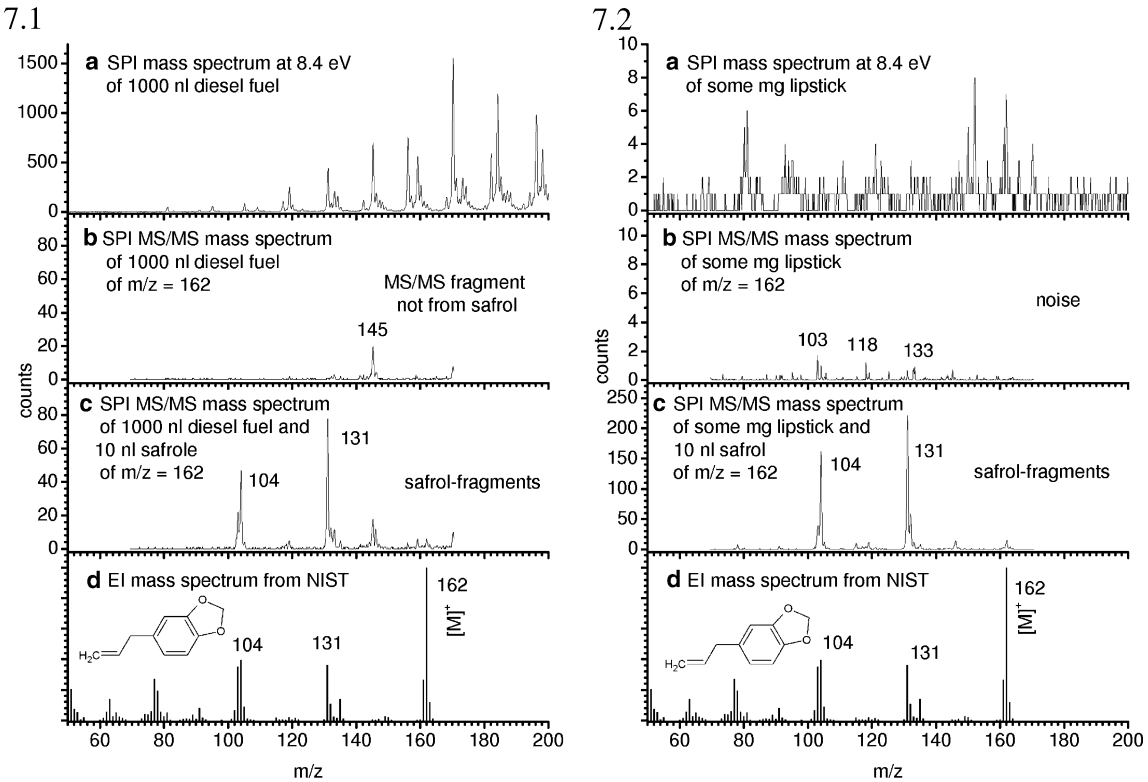

Fig. 7 Results of matrix measurements with safrole and different matrixes, *1* diesel-matrix, *2* lipstick-matrix

m/*z*=145. This results from a molecule with *m*/*z*=162 (as this is the mass for the MS/MS study) and the loss of fragment with *m*/*z*=17. This can be the loss of an OH-group, but it cannot be considered to originate from a safrole molecule, as that loss is not reasonable for safrole. Thus, this peak will not yield a false-positive signal.

In the next step, additionally to the matrix, 10 nl safrole, respectively, was added to the wipe pads and the measurement was repeated with the same settings. As a result, in Fig. 7.1c and 2c), the safrole fragments at *m*/*z*=131 and 104 are clearly visible. Thus, this matrix does not prevent the proper detection of safrole. Anyway, the signal from 10 nl safrole in 1 µl diesel fuel is slightly smaller than within the measurement with lipstick, but this is to be expected as diesel fuel is a rather difficult matrix.

In conclusion, the matrix-acceptance of the system is very good, as these common and difficult matrices do not yield false-positive or false-negative detection even at very high concentrations.

Results within the real-scenario measurement campaign

Additional to massive but still "artificial" matrixes, real trace detection of security-relevant substance offers another challenge. After the transportation to the point of use, the measurement system has to deal with uncontrolled environmental conditions during field operation. Thus, the system has to be robust enough to endure the transportation, high or low temperatures, humid or dry air, and dust. Also, it should be ready to use shortly after arriving and easy to operate.

For testing our setup within a real-scenario environment, the BKA enabled a measurement campaign within a former large-scale clandestine ecstasy laboratory. After its seizure within a privately used bunker facility in Germany, near the Dutch border, it has been preserved for training and education purposes. Although all drugs, precursors, solvents and chemicals have been removed from the place and the former clandestine lab has been cleaned, traces of MDMA were still expected to be present on the floor, walls and, especially, on and inside the laboratory equipment. The temperature was about 8 °C. So, this locality shown enables a rather real and challenging measurement scenario.

For the campaign, the TD-SPI-ITMS demonstrator was put into a small van and driven across Germany to the bunker facility. There, the van was parked right inside the bunker at a room separate from the chemical equipment. The measurements were performed with the setup still inside the van. That minimized the required site preparations before measurement, like turning on the vacuum pumps, computer, helium supply, and heater. Thus, the system was ready to use within about an hour. Within the bunker, wall plug electrical power supply was available. However, a generator or a high-power battery pack could

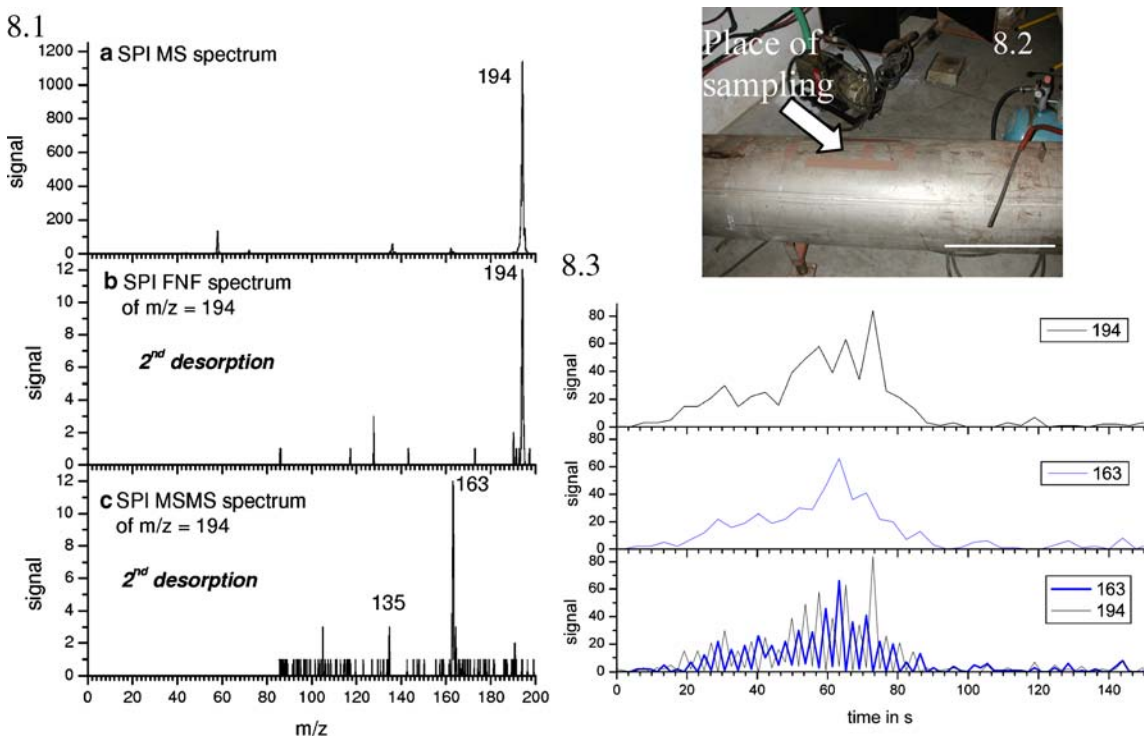

Fig. 8 Results of real-scenario measurement campaign within a clandestine MDMA laboratory, *1* SPI MS, FNF and MS/MS mass spectra of a real sample, *2* Equipment from which the samples for 1 and *2* were taken, *3* temporal profile of the SPI FNF and MS/MS measurement

easily be mounted into the van in order to make the system autonomous.

Within the bunker, samples were taken with wipe pad on the walls, the floor, and the surface of the reactors of the large-scale MDMA synthesis equipment. Therefore, 10× 10 cm squares were wiped with pads. These samples were taken to the TD-SPI-ITMS and measured onsite.

Figure 8.1 shows the mass spectra of one of these samples taken on the equipment shown in Fig. 8.2. Thereby, during the first desorption, the SPI mass spectrum shown in Fig. 8.1a was recorded showing nearly exclusively the molecular ion peak of MDMA at $m/z=194$. The signal was high enough so that it was possible to desorb the same pad a second time and to record FNF mass spectrum alternating with the MS/MS mass spectrum shown in Fig. 8.1b and c. These two measurements were accomplished alternately resulting in the temporal course of the peaks at $m/z=194$ and 163 shown in Fig. 8.3. This alternate temporal profile enhances the correlation of the MS/MS fragment at $m/z=163$ to originate from the peak at $m/z=194$. As even the MS/MS fragment at $m/z=135$ could be recorded, MDMA could clearly be identified on the wipe pad. For comparison, the SPI MS/MS mass spectrum of MDMA shown in Fig. 5.2c shows the same fragments. The ration of the fragments at $m/z=163$ and m/z=163 are slightly different. This is possibly due to the very low signal level in the spectrum recorded within the field measurement or due to matrix effects and do not prevent the identification.

Summarizing, this measurement campaign demonstrated successfully the field-suitability of the TD-SPI-ITMS system.

Outlook and conclusion

The results presented here show that it is possible to detect traces of security-relevant substances with thermal desorption–soft ionization–ion trap mass spectrometry within complex matrices. The matrix-acceptance of the system is very good, due to the soft ionization and the MS/MS technique applied. The detection limit was determined and is in an acceptable range for the first measurements. These proves the setup to be mobile, robust and field-suited.

Nevertheless, further developments are necessary in the future. Therefore, a follow-up project has already started. The development of the EBEL with increased photon density is a main task. It is planned to use another beam geometry and/or pulsed beam synchronized with the trap frequency to improve the sensitivity about more than one order of magnitude. Additionally, the thermal desorber has to be improved. Moreover, it is planned to add a Fourier-transform infrared spectrometer as an orthogonal detection method and for bulk detection as well as an endoscopic device for sampling in areas difficult to access. Additionally, solid-phase micro extraction sampling and laser desorption of explosives from surfaces will be applied. Furthermore, an enrichment of the samples prior to the mass spectrometer is planned to improve detection limits by at least a factor of three. The mass spectrometer will be exchanged, too. By using internal instead of external ionization, the trapping efficiency and thereby the detection limit will be improved by the factor of about two. And by using a supersonic jet inlet for cooling of the molecules prior to the ionization, fragmentation will be minimized. Thus, the molecular ion peak and therewith the sensitivity will improve, too.

Acknowledgements We gratefully acknowledge the funding of the project by the German Federal Ministry of Education and Research (BMBF) (FKZ 13N8820) and the good scientific cooperation with Varian Inc.

References

1. Hanson D (2005) Right in your backyard: identifying illegal drug labs lurking in the shadows. Law Enforc Technol 32:8–16
2. Pella PA (1977) Measurement of the vapor pressures of TNT, 2, 4-DNT, 2, 6-DNT, and EGDN. J Chem Thermodyn 9:301–305
3. Kanu AB, Hill HH, (2004). Ion Mobility Spectrometry: Recent Developments and Novel Applications. LabPlus International April/May: 20-26.
4. Jiménez AM, Navas MJ (2004) Chemiluminescence detection systems for the analysis of explosives. J Hazard Mater 106:1–8
5. Wise MB, CVT RM, Guerin MR (1997) Review of direct MS analysis of environmental samples. Field Anal Chem Technol 1:251–276
6. Yinon J (2002) Field detection and monitoring of explosives. TrAC, Trends Anal Chem 21:292–301
7. Bauer C, Sharma AK, Willer U, Burgmeier J, Braunschweig B, Schade W, Blaser S, Hvozdara L, Müller A, Holl G (2008) Potentials and limits of mid-infrared laser spectroscopy for the detection of explosives. Appl Phys, B Lasers Opt 92:327–333
8. Furton KG, Myers LJ (2001) The scientific foundation and efficacy of the use of canines as chemical detectors for explosives. Talanta 54:487–500
9. Nambayah M, Quickenden TI (2004) A quantitative assessment of chemical techniques for detecting traces of explosives at counter-terrorist portals. Talanta 63:461–467
10. Moore DS (2004) Instrumentation for trace detection of high explosives. Rev Sci Instrum 75:2499–2512
11. Steinfeld JI, Wormhoudt J, (1998). EXPLOSIVES DETECTION: A Challenge for Physical Chemistry. Annual Review of Physical Chemistry 49: 203 LP - 232.
12. Shi YJ, Lipson RH (2005) An overview of organic molecule soft ionization using vacuum ultraviolet laser radiation. Can J Chem 83:1891–1902
13. Butcher DJ (1999) Vacuum ultraviolet radiation for single-photoionization mass spectrometry: a review. Microchem J 62:354–362
14. March RE (1997) An introduction to quadrupole ion trap mass spectrometry. J Mass Spectrom 32:351–369
15. March JFJT RE (1995) Practical Aspects of Ion Trap Mass Spectrometry/ Fundamentals of Ion Trap Mass Spectrometry. CRC, New York

16. March RE, Hughes RJ (1989) Quadrupole storage mass spectrometry. Wiley, New York
17. Schramm E, Kuerten A, Hoelzer J, Mitschke S, Muehlberger F, Sklorz M, Wieser J, Ulrich A, Puetz M, Schulte-Ladbeck R, Schultze R, Curtius J, Borrmann S, Zimmermann R, (2009). Trace Detection of Organic Compounds in Complex Sample Matrixes by Single-Photon Ionization Ion Trap Mass Spectrometry: Real-Time Detection of Security-Relevant Compounds and Online Analysis of the Coffee-Roasting Process. Anal Chem 81(11):4456–4467.
18. Butcher DJ, Goeringer DE, Hurst GB (1999) Real-time determination of aromatics in automobile exhaust by single-photon ionization ion trap mass spectrometry. Anal Chem 71:489–496
19. Hanna SJ, Campuzano-Jost P, Simpson EA, Robb DB, Burak I, Blades MW, Hepburn JW, Bertram AK (2009) A new broadly tunable (7.4–10.2 eV) laser based VUV light source and its first application to aerosol mass spectrometry. Int J Mass Spectrom 279:134–146
20. Tsuruga S, Futami H, Yamakoshi H, Danno M, Yamashita I, Kuribayashi S (2004) Real-time measurement of trichlorobenzene of dioxin precursor in an incinerator exhaust by vacuum ultraviolet light ion trap/ionization TOFMS. J Mass Spectrom Soc Jpn 52:295–300
21. Kuribayashi S, Yamakoshi H, Danno M, Sakai S, Tsuruga S, Futami H, Morii S (2005) VUV single-photon ionization ion trap time-of-flight mass spectrometer for on-line, real-time monitoring of chlorinated organic compounds in waste incineration flue gas. Anal Chem 77:1007–1012
22. Tsuruga S, Suzuki T, Takatsudo Y, Seki K, Yamauchi U, Kuribayashi H, Morii S (2007) On-line Monitoring System of P5CDF Homologues in Waste Incineration Plants Using VUV-SPI-IT-TOFMS. Environ. Sci. Technol. 41:3684–3688
23. Short LC, Cai S-S, Syage JA (2007) APPI-MS: effects of mobile phases and VUV lamps on the detection of PAH compounds. J Am Soc Mass Spectr 18:589–599
24. Syage JA (2004) Mechanism of [M + H]+ formation in photoionization mass spectrometry. J Am Soc Mass Spectr 15:1521–1533
25. Andrea Raffaelli AS (2003) Atmospheric pressure photoionization mass spectrometry. Mass Spectrom Rev 22:318–331
26. Syage JA, Hanold KA, Lynn TC, Horner JA, Thakur RA (2004) Atmospheric pressure photoionization: II. Dual source ionization. J Chromatogr A 1050:137–149
27. Mullen C, Irwin A, Pond BV, Huestis DL, Coggiola MJ, Oser H (2006) Detection of explosives and explosives-related compounds by single photon laser ionization time-of-flight mass spectrometry. Anal Chem 78:3807–3814
28. Pond BV, Mullen C, Suarez I, Kessler J, Briggs K, Young SE, Coggiola MJ, Crosley DR, Oser H (2007) Detection of explosive-related compounds by laser photoionization time-of-flight mass spectrometry. Appl Phys, B Lasers Opt 86:735–742
29. El-Habachi A, Schoenbach KH (1998) Emission of excimer radiation from direct current, high-pressure hollow cathode discharges. Appl Phys Lett 72:22–24
30. Mühlberger F, Wieser J, Ulrich A, Zimmermann R (2002) Single photon ionization (SPI) via incoherent VUV-excimer light: robust and compact time-of-flight mass spectrometer for on-line, real-time process gas analysis. Anal Chem 74:3790–3801
31. Schramm E, Mühlberger F, Mitschke S, Reichardt G, Schulte-Ladbeck R, Pütz M, Zimmermann R (2008) Determination of the ionization potentials of security-relevant substances with single photon ionization mass spectrometry using synchrotron radiation. Appl Spectrosc 62:238–247
32. Mallard WG, Linstrom PJ, (2000). NIST Chemistry WebBook, NIST Standard Reference Database. http://webbook.nist.gov/chemistry: National Institute of Standards and Technology (NIST).
33. Saraji-Bozorgzad M, Geißler R, Streibel T, Mühlberger F, Sklorz M, Kaisersberger E, Denner T, Zimmermann R (2008) Thermogravimetry coupled to single photon ionization quadrupole mass spectrometry: a tool to investigate the chemical signature of thermal decomposition of polymeric materials. Anal Chem 80:3393–3403
34. Mühlberger F, Saraji-Bozorgzad M, Gonin M, Fuhrer K, Zimmermann R (2007) Compact ultrafast orthogonal acceleration time-of-flight mass spectrometer for on-line gas analysis by electron impact ionization and soft single photon ionization using an electron beam pumped rare gas excimer lamp as VUV-light source. Anal Chem 79:8118–8124
35. Ouyang Z, Noll RJ, Cooks RG (2009) Handheld miniature ion trap mass spectrometers. Anal Chem 81:2421–2425
36. Schnelle-Kreis J, Sklorz M, Peters A, Cyrys J, Zimmermann R (2005) Analysis of particle-associated semi-volatile aromatic and aliphatic hydrocarbons in urban particulate matter on a daily basis. Atmos Environ 39:7702–7714
37. Streibel T, Weh J, Mitschke S, Zimmermann R (2006) Thermal desorption/pyrolysis coupled with photo ionization time-of-flight mass spectrometry (PI-MS) for the analysis of molecular organic compounds as well as oligomeric and polygomeric fractions in urban particulate matter. Anal Chem 78:5354–5361
38. Mühlberger F, Streibel T, Wieser J, Ulrich A, Zimmermann R (2005) Single photon ionization time-of-flight mass spectrometry with a pulsed electron beam pumped excimer VUV lamp for on-line gas analysis: Setup and first results on cigarette smoke and human breath. Anal Chem 77:7408–7414
39. Williams BA, Tanada TN, Cool TA, (1992). Resonance Ionization Detection Limits for Hazardous Emissions. 24th Symposium (International) on Combustion. Pittsburgh: The Combustion Institute, 1587-1596.